ACOUSTICS 2012

A comparison between the performance of different silencer designs for gas turbine exhaust systems

R. Kirby[a], P. Williams[a] and J. Hill[b]

[a]Brunel University, Kingston Lane, Uxbridge, UB8 1PH Middlesex, UK
[b]AAF Ltd, Bassington Lane, Cramlington, NE23 8AF Northumberland, UK
ray.kirby@brunel.ac.uk

The dissipative silencers used to attenuate noise emanating from air moving devices such as fans are normally of a simple splitter design, with parallel baffles of absorbent material arranged over the width of a duct. However in more specialist applications, such as the exhaust systems of gas turbines, different silencer geometries are often used. One such geometry is a so-called bar silencer, in which rectangular bars, or bricks, of absorbing material are placed in a lattice arrangement over the duct cross section. The acoustic performance of these bar silencers is investigated here using a finite element based numerical mode matching scheme. The insertion loss of the bar silencers is then calculated and compared against traditional splitter designs in order to investigate the relative efficiency of each design

1 Introduction

Attenuating noise from fluid moving devices presents a considerable challenge. Normally considerations of space mean that large reactive based silencers are inappropriate and so attention inevitably turns to the use of sound absorbing materials. Traditionally, fibrous materials such as rock wool or glass fibre are used and these are arranged in parallel baffles to give the so-called splitter silencer configuration. These dissipative silencers are then placed upstream (intake) and downstream (exhaust) from the fluid moving device. The use of only of porous materials to attenuate sound does of course mean that these splitter silencers generally perform well at medium to high frequencies but are less effective at lower frequencies. This article examines in more detail the design of these silencers and investigates the effect of arranging the porous materials in an alternative “bar” or “brick” configuration in order to improve acoustic performance over a wide frequency range. To do this a mathematical model is developed and numerical experiments are carried out with the aim of investigating performance of silencers used on gas turbines.

Quantifying the performance of large dissipative silencers is challenging. The measurement of these silencers according to European Standards [1] requires very expensive testing equipment and although some experimental data has been reported for silencer transmission loss (for example, Kirby et al. [2]) there is very little data available in the literature. In view of this, focus has turned to developing theoretical models, which allow for relatively quick and easy investigations into silencers deigns to be performed when compared to experimental testing. Here, the most popular methods for characterising silencer performance have traditionally been based on computing modal attenuation, usually the least attenuated mode, see for example references [3] – [7]. However, these models do not take into account the scattering of sound from the inlet and outlet planes. It is only recently that these effects have been fully characterised for splitter silencers and here Lawrie and Kirby [8], and Kirby [9] used numerical and analytic methods to compute silencer insertion/transmission loss for those silencers typically found in air conditioning ducts. Here, the method of Kirby [9] is the most appropriate for studying the insertion loss of silencers with a more general design since the numerical approach facilitates the study of arbitrary cross-sectional geometries, whilst also accommodating perforated plates and fairings that are typically found in both the intake and exhaust of gas turbine silencers. Accordingly, the method reported by Kirby [9] is used here to investigate alternative silencer designs to those traditionally used and this will focus on the study of bar silencers similar to those studied by Cummings and Astley; however, this article will proceed to analyse the insertion loss of these bar silencer, rather than restrict the analysis to modal attenuation. Predictions will also be compared to a simple splitter silencer in order to review the relative performance of each design. The theory is presented first in the following section, results are then presented in section 3 and finally conclusions are draw regarding the relative acoustic performance of the two types of silencer.

2 Theory

The dissipative silencer is assumed to be uniform in length, but to have an arbitrary cross section containing a region of porous material R_m, surrounded by a region of fluid R_F. The cross section of the silencer is shown in Figure 1.

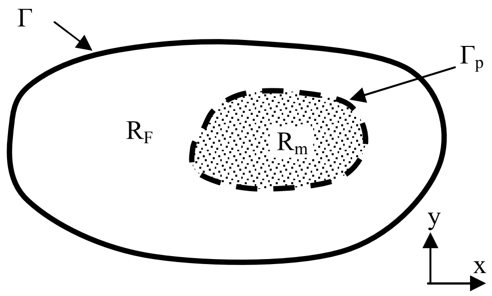

Figure 1: Cross sectional geometry of general dissipative silencer.

For reasons of clarity only one region of porous material is shown in Figure 1, although the analysis that follows is completely general and it is assumed that region R_m may be further separated into additional regions of porous material in order to take on the geometry of, say, a parallel baffled splitter silencer or a bar silencer. In addition, Γ_p denotes a perforate separating the fluid from the porous material and Γ_F denotes the outer surface of the silencer, which is assumed to be a hard wall and may also take on the outer surface of R_m. The geometry in the axial direction is shown in Figure 2.

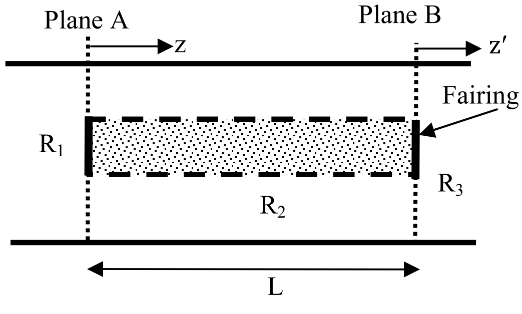

Figure 2: Axial geometry of uniform dissipative silencer.

In Figure 2, a plane wave is assumed to be incident from the left, in region R_1. The splitter silencer and the fluid region is grouped together so that $R_2 = R_F + R_m$; the silencer is terminated anechoically in region R_3 so no reflected waves are permitted in this region. Finally, the inlet plane A, and the outlet plane B, denote the location of the silencer fairings, which are present at the entrance and exit to the silencer.

The acoustic wave equation for each region is given as

$$\frac{1}{c_q^2}\frac{\partial^2 p_q}{\partial t^2} - \nabla^2 p_q = 0. \quad (1)$$

Here, p_q is the acoustic pressure, and c is the speed of sound in region q, respectively; t is time. The solution now proceeds by first calculating the eigenmodes for the silencer cross section and then using point collocation to matching continuity of pressure and acoustic particle velocity over planes A and B. Accordingly, the sound pressure in each region is first expanded as an infinite sum over the duct eigenmodes, to give

$$p_1(\mathrm{x,y,z}) = \sum_{j=0}^{\infty} F_j \Phi_j(\mathrm{x,y})\mathrm{e}^{-\mathrm{i}k_0\gamma_j \mathrm{z}} + \sum_{j=0}^{\infty} A_j \Phi_\mathrm{j}(\mathrm{x,y})\mathrm{e}^{+\mathrm{i}k_0\gamma_j \mathrm{z}} \quad (2)$$

$$p_2(\mathrm{x,y,z}) = \sum_{m=0}^{\infty} B_m \Psi_m(\mathrm{x,y})\mathrm{e}^{-\mathrm{i}k_0\lambda_m \mathrm{z}} + \sum_{m=0}^{\infty} C_m \Psi_m(\mathrm{x,y})\mathrm{e}^{+\mathrm{i}k_0\lambda_m \mathrm{z}} \quad (3)$$

$$p_3(\mathrm{x,y,z'}) = \sum_{n=0}^{\infty} D_n \Phi_n(\mathrm{x,y})\mathrm{e}^{-\mathrm{i}k_0\gamma_n \mathrm{z'}} \quad (4)$$

Here, A_j, B_m, C_m, D_n, and F_j are modal amplitudes, λ_m, is the wavenumber in region R_2 and γ_j, is the wavenumber in the inlet/outlet section. The quantities $\Phi(\mathrm{x,y})$ and $\Psi(\mathrm{x,y})$ are the transverse duct eigenfunctions in the inlet/outlet region and the silencer section respectively. In addition $\mathrm{i} = \sqrt{-1}$ and $k_0 = \omega/c_0$.

On substituting the modal expansion for the each region into the governing wave equation, an eigenequation is obtained for regions R_1, R_2 and R_3. Here, regions R_1 and R_3 are assumed to be identical and an eigenequation may be found by implementing the hard wall boundary condition of $\nabla p \cdot \boldsymbol{n} = 0$ over Γ. This problem is solved using finite elements and has been repeated many times in the literature [8, 9] and so is not discussed further here. For the silencer section, one may arrive at an eigenequation by also enforcing continuity of velocity over the perforate, and for the pressure enforcing

$$p_\mathrm{m} - p_F = \rho_0 c_0 \zeta \boldsymbol{u}_m \cdot \boldsymbol{n}_m. \quad (5)$$

where, ζ is the (dimensionless) impedance of the perforate and u is the acoustic particle velocity. An eigenequation may then be constructed and it is solved here using the finite element method. See papers by Kirby and Lawrie [8], Kirby [9-11] for examples of how this eigenproblem is solved using the finite element method. Note that this eigenequation will contain the acoustic properties of the porous material, via the complex sound speed c_m and the complex density $\rho(\omega)$, which appears following the application of continuity of velocity between the fluid and the material. Values for these parameters may be specified by using Delany and Bazley coefficients [12] and this is discussed in more detail in the majority of the references included here.

On obtaining the eigenvalues λ_m and γ_j, and the eigenvectors $\Phi(\mathrm{x,y})$ and $\Psi(\mathrm{x,y})$ the silencer insertion loss may then be computed. To do this it is necessary to enforce continuity of acoustic pressure and normal particle velocity over planes A and B. This is accomplished here by using point collocation, which requires the pressure in each region to be written as a vector, which and this holds the values of pressure at each node in the finite element mesh. Thus, in vector form we may write the pressure as

$$\boldsymbol{p}_1(\mathrm{x,y,z}) = \sum_{j=0}^{n_1} F_j \boldsymbol{\Phi}_j(\mathrm{x,y})\mathrm{e}^{-\mathrm{i}k_0\gamma_j \mathrm{z}} + \sum_{j=0}^{n_1} A_j \boldsymbol{\Phi}_\mathrm{j}(\mathrm{x,y})\mathrm{e}^{+\mathrm{i}k_0\gamma_j \mathrm{z}} \quad (6)$$

$$\boldsymbol{p}_2(\mathrm{x,y,z}) = \sum_{m=0}^{n_2} B_m \boldsymbol{\Psi}_m(\mathrm{x,y})\mathrm{e}^{-\mathrm{i}k_0\lambda_m \mathrm{z}} + \sum_{m=0}^{n_2} C_m \boldsymbol{\Psi}_m(\mathrm{x,y})\mathrm{e}^{+\mathrm{i}k_0\lambda_m \mathrm{z}} \quad (7)$$

$$\boldsymbol{p}_3(\mathrm{x,y,z'}) = \sum_{n=0}^{n_1} D_n \boldsymbol{\Phi}_n(\mathrm{x,y})\mathrm{e}^{-\mathrm{i}k_0\gamma_n \mathrm{z'}} \quad (8)$$

where the modal sums have also been truncated at the numbers of nodes in the transverse finite element mesh in each region ($n_1 = n_3$). The modal amplitudes are no found by enforcing the following matching conditions over plane A,

$$\boldsymbol{p}_1(x,y,0) = \boldsymbol{p}_2(x,y,0) \quad \text{over } R_F \quad (9)$$

$$\boldsymbol{u}_1(x,y,0) = \boldsymbol{u}_2(x,y,0), \quad \text{over } R_F \quad (10)$$

$$\boldsymbol{u}_1(x,y,0) = 0, \quad \text{over } R_m \quad (11)$$

$$\boldsymbol{u}_2(x,y,0) = 0, \quad \text{over } R_m \quad (12)$$

and over plane B,

$$\boldsymbol{p}_2(x,y,L) = \boldsymbol{p}_3(x,y,0) \quad \text{over } R_F \quad (13)$$

$$\boldsymbol{u}_2(x,y,L) = \boldsymbol{u}_3(x,y,0), \quad \text{over } R_F \quad (14)$$

$$\boldsymbol{u}_2(x,y,L) = 0, \quad \text{over } R_m \quad (15)$$

$$\boldsymbol{u}_3(x,y,0) = 0. \quad \text{over } R_m \quad (16)$$

On substituting equations (6)- (8) into equations (9) to (16) one obtains a complete set of $n_t = 2(n_1 + n_2)$ simultaneous equations. After setting $F_0 = 1$, and $F_j = 0$ for $j > 0$ (plane wave excitation) then equations (9) to (16) may be solved for the unknown modal amplitudes. The silencer insertion Loss IL (or transmission loss, which is the same under these conditions) is then defined as

$$\mathrm{IL} = -10\log_{10} \mathrm{Re}\left[\sum_{n=0}^{n_1} \frac{\gamma_n I_n |D_n|^2}{I_0}\right], \quad (17)$$

where $I_n = \int_{R_1} |\Phi_n(\mathrm{x,y})|^2 \, dxdy$.

3 Results and Discussion

The numerical model described in the previous section is used here to analyse two different silencer designs: the splitter silencer typically used in air conditioning systems, and the bar-silencer which has found use in a number of applications but in this study its relevance to the exhaust systems of gas turbines is of most interest. This is of particular interest because the improved airflow distribution profile, and reduction in thermal stresses, can lead to improved equipment longevity and engine efficiency. In order to properly compare the two designs, the same percentage open area is chosen for both designs, and here values for open area of Δ = 75%, 50% and 25% are chosen. In Figures 3 and 4, the different silencer geometries are shown, where for the bar-silencer a square geometry is specified for ease of comparison, although any other cross-sections may readily be accommodated.

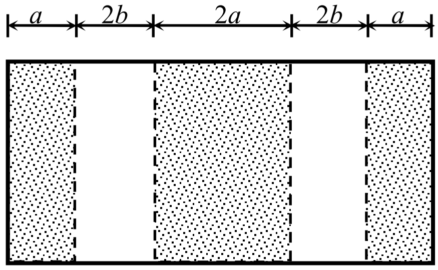

Figure 3: Geometry of splitter silencer

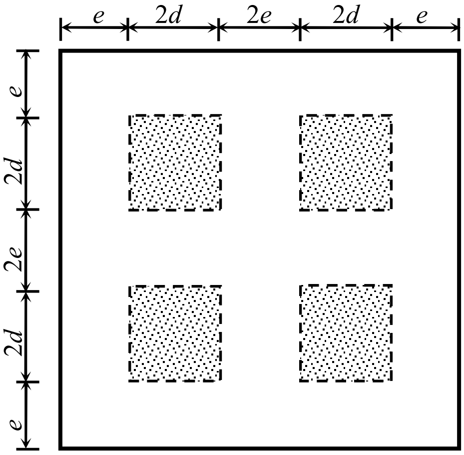

Figure 4: Geometry of bar-silencer

For the splitter silencer symmetry allows the eigenvalue problem to be reduced to a one dimensional transverse finite element mesh, provided that a plane wave is incident on the silencer. However, for the bar silencer it is necessary to specify a two dimensional transverse finite element mesh, although symmetry does allow for the discretisation of only one quarter of the geometry shown in Figure 4. Therefore, the study of the bar silencer is considerably more computationally expensive than that of the splitter silencer under plane wave conditions.

In Figure 5 the insertion loss for splitter and bar silencers is compared for a silencer of length $L = 1$ m and open area $\Delta = 75\%$. In addition, $a = 0.05$ m, $b = 0.15$ m, $d = 0.1$ m, and $e = 0.1$ m, so the overall cross-sectional dimension of the bar-silencer is $0.8\text{ m} \times 0.8\text{ m}$. The flow resistivity of the porous material is 15,000 Pa s/m^2, the porosity of the perforate is 30%, the thickness of the perforated screen is 1.6 mm with a hole diameter of 3 mm. The solution for the splitter silencer is obtained using values of n_t up to a maximum of $n_t = 264$, whereas for the bar silencer as maximum value of $n_t = 1492$ was used.

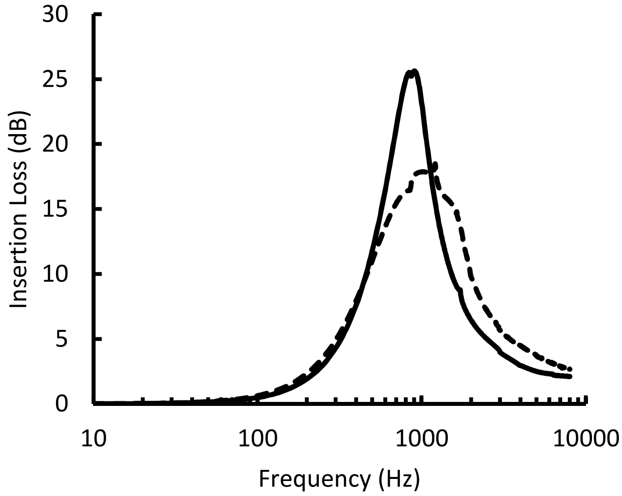

Figure 5: Insertion loss for an open area of Δ = 75%. ——— splitter silencer; – – – , bar silencer.

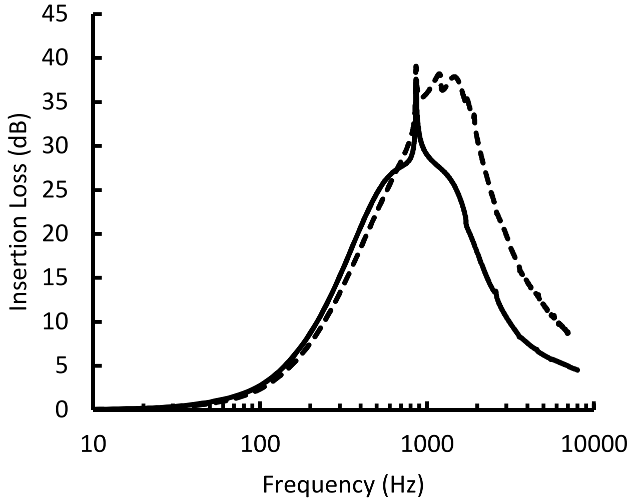

Figure 6: Insertion loss for an open area of Δ = 50%. ——— splitter silencer; – – – , bar silencer.

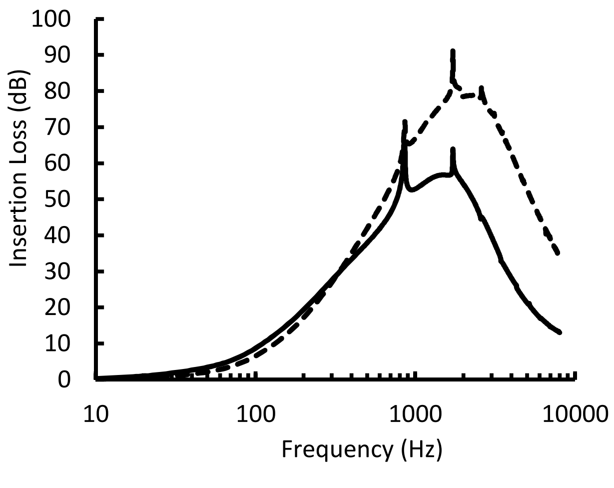

Figure 7: Insertion loss for an open area of Δ = 25%. ——— splitter silencer; – – – , bar silencer.

In Figure 6 the silencer insertion loss is plotted for $\Delta = 50\%$ ($a = 0.05$ m, $b = 0.15$ m, $d = 0.1$ m, and $e = 0.1$ m) and in Figure 7 for $\Delta = 25\%$ ($a = 0.05$ m, $b = 0.15$ m, $d = 0.1$ m, and $e = 0.1$ m), with all other variable stating the same.

In Figures 8-10, the same silencers are studied, but this time the flow resistivity of the porous material is changed to 50,000 Pa s/m^2.

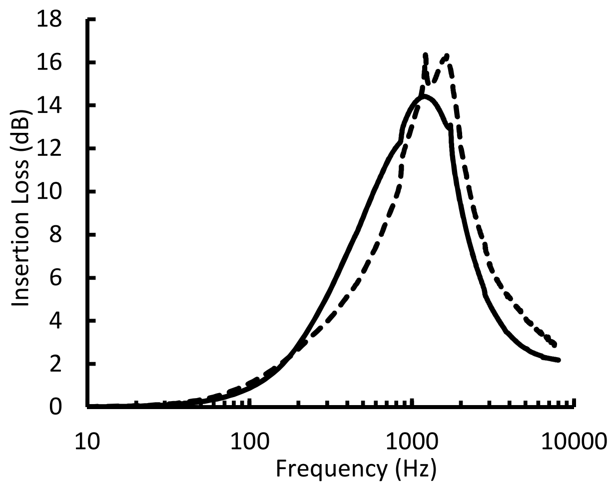

Figure 8: Insertion loss for an open area of Δ = 75%. ——— splitter silencer; – – – , bar silencer.

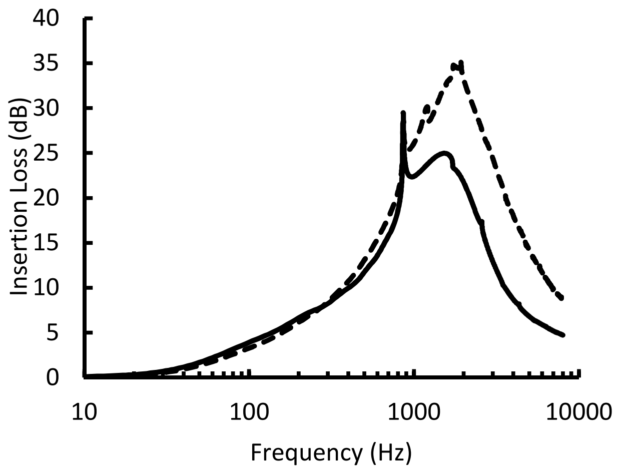

Figure 9: Insertion loss for an open area of Δ = 50%. ——— splitter silencer; – – – , bar silencer.

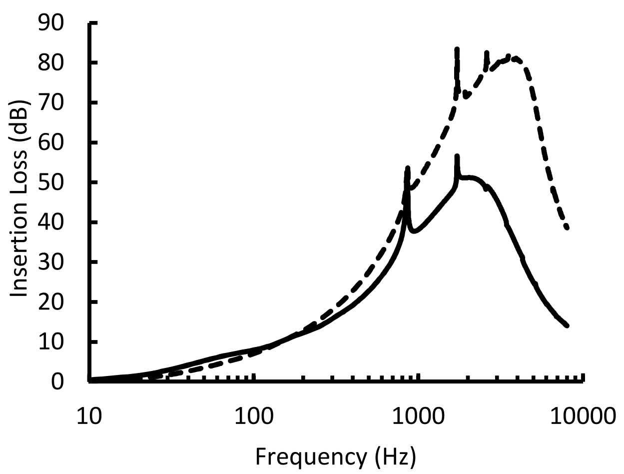

Figure 10: Insertion loss for an open area Δ = 25%. ——— splitter silencer; – – – , bar silencer.

It is clear from the plots in Figures 5-10 that the configuration in which the absorbing material is placed within the duct plays a significant role in silencer performance. For low percentage open areas the performance of the splitter and the bar silencer is similar, although the splitter silencer does tend to perform better at lower frequencies. But as the percentage open area is reduced the bar silencer becomes much more effective at higher frequencies. Whilst this is at the expense of a small drop in IL at lower frequencies the improvement in IL above about 1 kHz is very noticeable, both for $\Delta = 50\%$ and $\Delta = 25\%$. Of course, in reality one would not be able to achieve the IL levels seen in Figures 7 and 10 because noise flanking transmission would serve to reduce the IL values above about 60 dB. Nevertheless the improvement in IL is significant and is achievable for large open areas over a wide upper frequency range.

A large improvement in the performance of bar silencers, when compared to splitter silencers, was also observed by Nilsson and Söderqvist [13] who used experimental measurements to investigate the two different designs. Nilsson and Söderqvist quote a high frequency improvement of 35 dB, as well as a low frequency improvement of 4 dB. The theoretical results presented here tend not to support the claims for improvement in IL at lower frequencies, in fact for most of the bar silencers there is a small drop in IL. But at higher frequencies the effect of changing from a splitter to a bar silencer is clearly evident and supports the observations of Nilsson and Söderqvist, although this does depend on the percentage open area. Unfortunately it is not possible to compute the percentage open area of the silencer studied by Nilsson and Söderqvist, but it is probably reasonable to conclude that this was below 50% in view of the results presented here. Cummings and Astley [7] also studied a bar silencer and they examined three different percentage open areas: 36%, 55.6% and 66.7%. Cummings and Astley did not notice a significant increase in silencer performance in their predictions at higher frequency, and their experimental measurements are inconclusive. However, the predictions of Cummings and Astley are based on computing the least attenuated mode only and so at higher frequencies their model is likely to be inaccurate in view of the large number of higher order modes that will be propagating at these frequencies. Thus, the results presented here seem to support those observations of Nilsson and Söderqvist, but do not fully agree with the observations of Cummings and Astley [7]; there appears to be a case then for further experimental measurements to investigate the effect of the open area on silencer performance and to see if the predictions presented here provide a reliable indication of the relative performance of each design.

In Figure 11 the effect of flow resistivity on the performance of the bar silencer is investigated. Here, three flow resistivites are investigated: 10 kPa s/m^2, 30 kPa s/m^2 and 50 kPa s/m^2. It can be seen that as the flow resistivity of the porous material is increased the low to medium frequency performance of the bar silencer tends to drop, whereas the higher frequency performance does the opposite. It is noticeable, however, that the improvement in the low frequency performance is significant, whereas for higher frequencies the difference is less pronounced. Thus, the performance of the bar silencer is observed to be very dependent on the material chosen and the flow resistivity of this material (which is linked to the overall bulk density of the material placed in the silencer). This places a strong emphasis on the development of accurate design tools suitable for optimising silencer performance for a particular application.

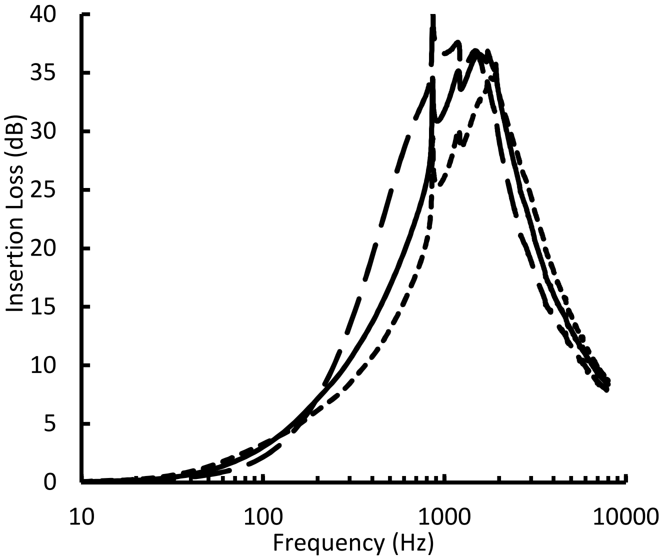

Figure 11: Insertion loss for a bar silencer of open area of Δ = 50%. — — — $\sigma = 10\ \mathrm{kPa\ s/m^2}$; ——— , $\sigma = 30\ \mathrm{kPa\ s/m^2}$, - - - $\sigma = 50\ \mathrm{kPa\ s/m^2}$

5 Conclusion

A finite element based mathematical model has been presented here, which is suitable for computing the insertion loss of a dissipative silencer of arbitrary (but uniform) cross-section. The model is used to investigate the relative performance of splitter and bar silencers. For a fixed percentage open area, significant differences between the performance of the two silencer designs is observed. This difference is most obvious as the percentage open area of each silencer is reduced, and here a significant improvement in performance at high frequencies is observed for the bar silencer. At lower frequencies the performance of the two silencer designs is observed to be similar. It is also shown the flow resistivity of the porous material used to fabricate the silencer play a significant role in silencer performance and needs to be chosen carefully for a particular application.

Acknowledgments

The authors would like to thank the UK Technology Strategy Board (TSB), through the Knowledge Transfer Programme (KTP), for their support of the work reported in this article.

References

[1] European Standard EN ISO 7235, "Measurement procedures for ducted silencers – insertion loss, flow noise and total pressure loss", (2003)

[2] R. Kirby, D. Herries, K. Amott, "Validating insertion loss predictions for HVAC silencers", *Proc. ICSV 16*, Kraków, Poland, July 2009.

[3] A. Cummings, "Sound attenuation in ducts lined on two opposite walls with porous material, with some application to splitter", *J. Sound Vib.* 49, 9-35 (1976).

[4] A. Cummings and N. Sormaz, "Acoustic attenuation in dissipative splitter silencers containing mean fluid flow", *J. Sound Vib.* 168, 209-227 (1993).

[5] R. Ramakrishnan and W. R. Watson, "Design curves for rectangular splitter silencers", *Appl. Acoust.* 35, 1-24 (1992).

[6] R. Ramakrishnan and R. Stevens, "Improving the accuracy of duct insertion loss predictions", *J. Sound Vib.* 169, 423-427 (1994).

[7] A. Cummings and R. J. Astley, "Finite element computation of attenuation in bar-silencers and comparison with measured data", *J. Sound Vib.* 196, 351-369 (1996).

[8] R. Kirby and J. B. Lawrie, "A point collocation approach to modelling large dissipative silencers", *J. Sound Vib.* 286, 313-319 (2005).

[9] R. Kirby, "The influence of baffle fairings in the acoustic performance of rectangular splitter silencers", *J. Acoust. Soc. Am.* 118, 2302-2312 (2005)

[10] R. Kirby, "Transmission loss predictions for dissipative silencers of arbitrary cross section in the presence of mean flow", *J. Acoust. Soc. Am.* 114, 200-209 (2003)

[11] R. Kirby, "A comparison between analytic and numerical methods for modelling automotive dissipative silencer with mean flow", *J. Sound Vib.* 325, 565-582 (2009).

[12] M. E. Delany and E. N. Bazley, "Acoustical properties of fibrous materials", *Appl. Acoust.* 3, 105-116 (1970)

[13] N-Å. Nilsson and S. Söderqvist, "The bar silencer – improving attenuation by constricted two dimensional wave propagation", *Proc. Inter-Noise* 83, 1-4, (1983).